

and Antibacterial Properties in the Setting of MRSA

Erin Baker, PhD^{1,2,5}; Corinn Gehrke, BS¹; Matthew Siljander, MD³; Jonathan Wright, MD³; Kimberly Powell, BS⁴; Mackenzie Fleischer, MS¹; Samantha Hartner, MS¹; Michael Newton, MS¹; Matthew Sims, MD, PhD⁴; Paul Fortin, MD³; Craig Friedrich, PhD⁵

¹ Department of Orthopaedic Research, Beaumont Health, Royal Oak, MI
² Oakland University William Beaumont School of Medicine, Rochester, MI
³ Department of Orthopaedic Surgery, Beaumont Health, Royal Oak, MI
⁴ Department of Infectious Diseases Research, Beaumont Health, Royal Oak, MI
⁵ Department of Mechanical Engineering, Michigan Technological University, Houghton, MI



INTRODUCTION

Periprosthetic joint infection (PJI) remains a challenging complication that may lead to multiple revision surgeries, increased healthcare cost, long-term disability, and increased mortality. Titania nanotube (TiNT) surfaces have previously shown increased bone-implant contact area, enhanced *de novo* bone formation on and adjacent to the implant as well as higher pull-out forces (increased osseointegration), compared to non-textured controls.

PURPOSE

In this study, the antibacterial properties of TiNT surfaces, TiNT surfaces integrated with nanosilver, and two current standard-of-care materials (titanium thermal plasma sprayed and titanium alloy surfaces) were evaluated.

METHODS

All experiments were performed after obtaining approval from the Institutional Biosafety and Institutional Animal Care and Use Committees. Coupon (12 mm x 12 mm) and implant (4 mm x 20 mm cylindrical) samples were prepared according to previous published methods.[1] TiNT surfaces with nanotube diameters of 60nm, 80nm, 110nm, and 150nm were prepared (Figure 1). Hybrid electrolytes were used to integrate nanosilver (TiNT+Ag) with silver concentrations among the nanotubes of ~1ppm to 8ppm. Titanium alloy (Ti; Ti6Al4V) and thermal plasma sprayed (TPS) surfaces were used as-is.

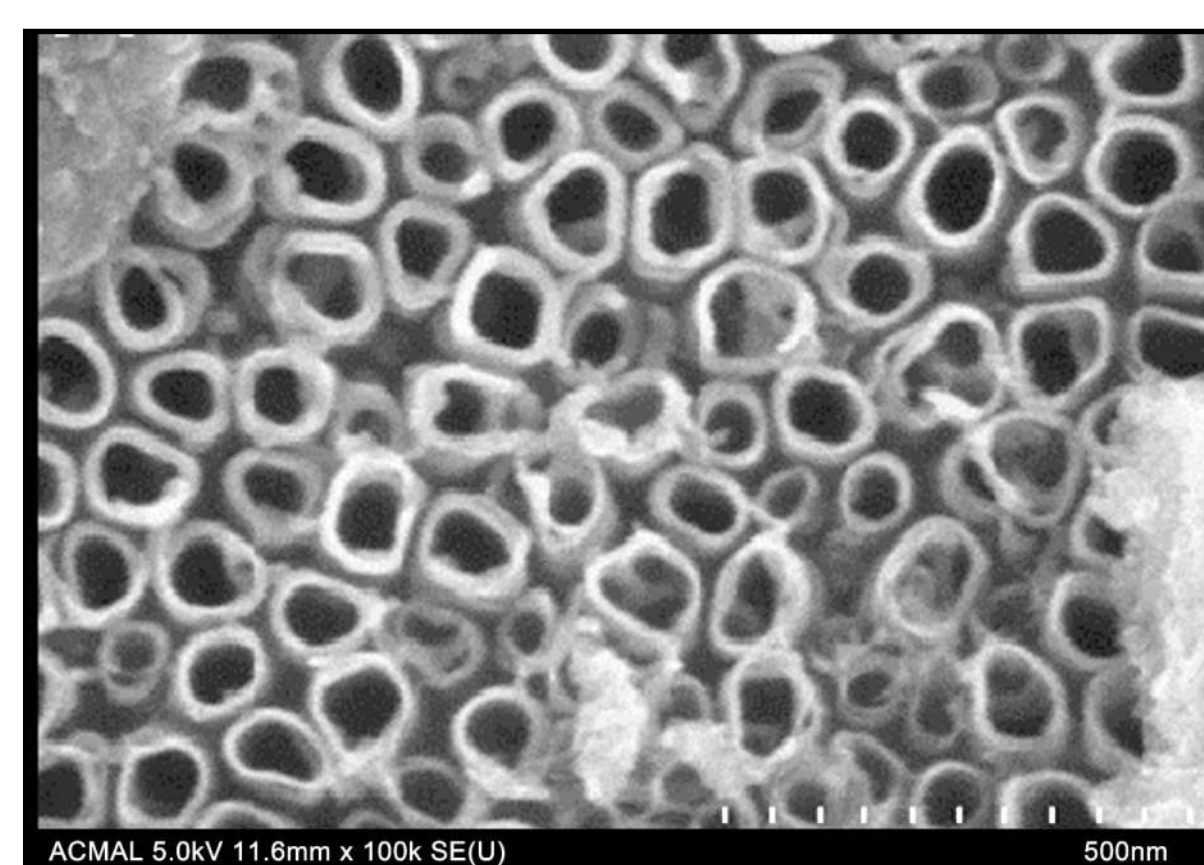


Figure 1. Representative image of a nanotube surface with 80 nm diameter nanotubes.

In a follow-on *in vivo* study, anesthetized New Zealand White rabbits (female, retired breeder) underwent bilateral antegrade implantation of an intramedullary tibial implant with one of four materials (TiNT, TiNT+Ag, TPS, Ti). For nanotube surfaces, selected diameter was the “best performer” from *in vitro* work (n=12 animals per groups; 2-week endpoint). In one tibia, a human clinical isolate of MRSA (10⁵ CFU/mL) in LB broth was introduced to the implant, then covered with sterile bone wax. In the other tibia, LB broth (no MRSA) was introduced into the contralateral tibia and covered with sterile bone wax. In each group, six animals were randomized to sonication analysis (i.e. implants were removed from each tibiae and sonicated in sterile phosphate buffered saline to quantify viable bacteria from the implant surface) and six animals were randomized to imaging analysis. Specifically, analysis of a volume of interest (epiphysis to distance of 10 mm) surrounding the implant at the proximal tibia via high-resolution microcomputed tomography (μ CT, vivaCT 80,

Scanco USA) (osseointegration) and nondecalcified histology processing (gram-staining to assess bacteria with retained implant and Stevenel’s Blue to assess bone formation) were performed. μ CT results were statistically compared using t-tests (no correction for multiple comparisons). Gram-stained sections were histologically analyzed through a custom MATLAB (V9.5, Mathworks) program to randomize six ROIs and quantify gram-positive bacteria at the bone-implant interface. An additional therapeutic cohort of rabbits, n=12, underwent the same process with infection development for 4 days prior to vancomycin treatment for 7 days until endpoint. In each implant group, the same analysis was performed for sonication (n=2 animals) and histology and imaging (n=1 animal).

RESULTS

The first *in vitro* experiment indicated that none of the material surfaces were able to kill MRSA in the surrounding LB broth; however, the second experiment showed lower MRSA counts on the TiNT groups at all timepoints and on the TiNT+Ag group at the 24 hr and 48 hr timepoints. All of the TiNT surfaces had significantly less viable MRSA than TPS at each of the timepoints. In the *in vivo* experiment, the 110 nm diameter TiNT were selected for the implants as the surfaces had the least amount of viable MRSA compared with the other diameters; 110 nm diameter TiNT were also used for the TiNT+Ag implants.

Sonication analysis indicated that viable MRSA was greater on the TiNT and TiNT+Ag surfaces (~10⁴ CFU/ml) vs. the Ti and TPS surfaces (~10³ CFU/ml); however, both TiNT and TiNT+Ag had one sample with 0 CFU/ml (confirmed with an additional 24 hr incubation), while one TPS sample had 0 CFU/ml but subsequently grew colonies after an additional 24 hr incubation (Table 1).

Table 1. Viable MRSA after implant sonication; μ CT imaging analysis of bone formation (bone-implant contact, bone volume fraction, and tissue mineral density); and histologic analysis of bone formation and bacteria at implant interface (bone-implant contact, gram positive percentage) for both the non-treatment (left column) and treatment (right column) cohorts.

| Implant Sonication Analysis (n=6, per group) | | | | | Implant Sonication Analysis, Treatment Cohort (n=2, per group) | | | | |
|--|--------------------|------------------------|--|--|--|--------------------|--------------------|--------------------|--|
| Group | Avg. MRSA (CFU/mL) | Rng. MRSA (CFU/mL) | | | Group | Avg. MRSA (CFU/mL) | Min. MRSA (CFU/mL) | Max. MRSA (CFU/mL) | |
| TiNT | 1.58 E+04 | 0.00 E+00 to 3.35 E+04 | | | TiNT | 2.69 E+03 | 1.11 E+03 | 4.26 E+03 | |
| TiNT+Ag | 3.84 E+04 | 0.00 E+00 to 2.00 E+05 | | | TiNT+Ag | 4.56 E+02 | 9.00 E+01 | 8.22 E+02 | |
| Ti | 3.72 E+03 | 3.25 E+03 to 8.14 E+03 | | | Ti | 1.47 E+03 | 3.70 E+02 | 2.56 E+03 | |
| TPS | 2.57 E+03 | 0.00 E+00 to 4.84 E+03 | | | TPS | 8.69 E+03 | 3.88 E+03 | 1.35 E+04 | |

| Imaging Analysis (n=6, per group) | | | | | Imaging Analysis, Treatment Cohort (n=1, per group) | | | | |
|-----------------------------------|---------------|---------------|---------------|--|---|---------|-------|----------|--|
| Group | BIC (%) | BV/TV | TMD (HU) | | Group | BIC (%) | BV/TV | TMD (HU) | |
| TiNT | 1.183 ± 0.393 | 1.002 ± 0.270 | 0.958 ± 0.033 | | TiNT | 1.028 | 0.866 | 0.966 | |
| TiNT+Ag | 1.625 ± 0.586 | 1.006 ± 0.247 | 0.960 ± 0.025 | | TiNT+Ag | 0.754 | 0.990 | 0.970 | |
| Ti | 1.164 ± 0.561 | 0.881 ± 0.199 | 0.857 ± 0.043 | | Ti | 0.739 | 0.924 | 0.978 | |
| TPS | 0.986 ± 0.208 | 1.352 ± 0.836 | 0.973 ± 0.034 | | TPS | 1.168 | 1.021 | 1.005 | |

| Histologic Section Analysis (n=6, per group) | | | | | Histologic Section Analysis, Treatment Cohort (n=1, per group) | | | | |
|--|---------|--------------|--------|-------------|--|---------|--------------|--------|-------------|
| Group | BIC (%) | Rng. BIC (%) | GP (%) | Rng. GP (%) | Group | BIC (%) | Rng. BIC (%) | GP (%) | Rng. GP (%) |
| TiNT | 33 | 12-53 | 13 | 1-26 | TiNT | 9 | | 5 | |
| TiNT+Ag | 41 | 19-60 | 9 | 3-14 | TiNT+Ag | 24 | | 15 | |
| Ti | 12 | 3-28 | 6 | 2-13 | Ti | 15 | | 3 | |
| TPS | 15 | 0-34 | 10 | 3-21 | TPS | 16 | | 8 | |

Greatest bone-implant contact (BIC from μ CT) in infected limbs was on TPS implants, followed by TiNT, TiNT+Ag, and Ti (Table 1). BIC was significantly greater in TiNT+Ag vs. TPS implants (p=0.030). In the TC, BIC% was greatest in the TPS group, followed by the TiNT group and approximately equivalent in the Ti and TiNT+Ag groups. Analysis of

histologic sections (Figure 2) showed TiNT+Ag had the greatest average BIC%, followed by TiNT, Ti, and TPS. In the TC, BIC% was greatest in TiNT+Ag implants, followed by TPS, Ti, and TiNT. Ti had the lowest average GP%, followed by TiNT+Ag, TPS, and TiNT. In the TC, Ti had the lowest GP%, followed by TiNT, TPS, and TiNT+Ag (Table 1).

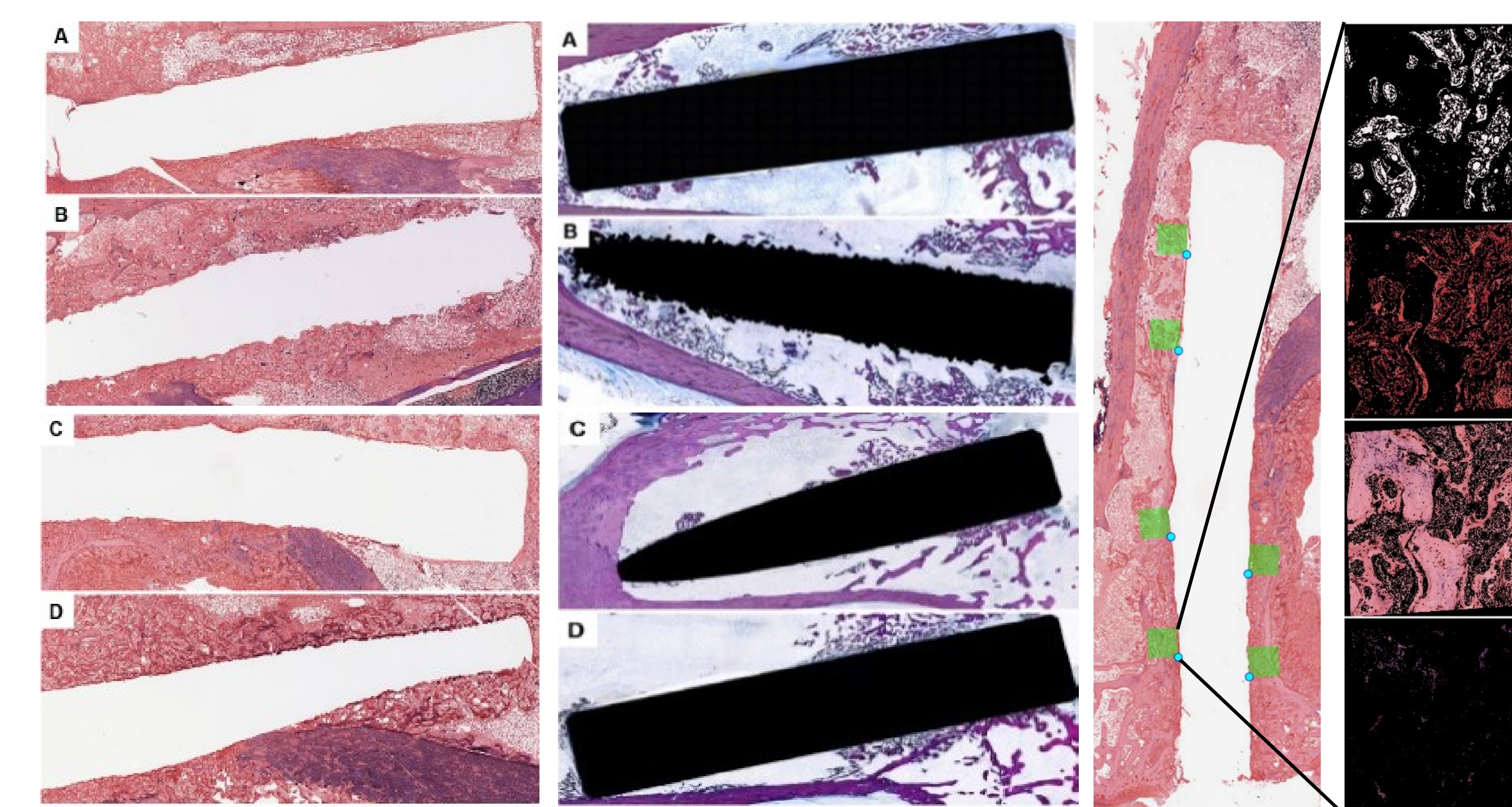


Figure 2. Representative histologic sections of Gram-stained sections (left column) and Stevenel’s Blue-stained sections (middle column) of infected Ti (A), TPS (B), TiNT (110 nm diameter) (C), and TiNT+Ag (110 nm diameter) (D). Histologic section of Gram-stained infected tibia with randomly selected standard-sized regions of interest along the bone-implant interface with segmentation of region of interest (right column with inset images).

CONCLUSIONS

Results from *in vitro* drop-seeding experiments indicated that TiNT and TiNT+Ag surfaces were more efficacious in resisting MRSA biofilm formation compared to Ti and TPS surfaces. Sonication analysis indicated that TPS and Ti implants had less viable bacteria; however, overnight incubations showed that the implants continued to grow bacteria after sonication, perhaps indicating that differential adhesion of bacteria to the various surfaces may have interfered with assessment of true *in vivo* antimicrobial efficacy. Specifically, the authors hypothesize that during sonication, bacterial detaches more readily from TiNT surfaces than from TPS and Ti surfaces, resulting in increased viable MRSA in the sonicate of TiNT implants compared with sonicate from TPS and Ti implants. Osseointegrative properties, measured by μ CT, in the setting of infection were greatest in TPS implants. With a reduction in viable bacteria from nanotube surfaces following antibiotic treatment, MRSA clearance rates may improve with the NT surface modification. Osseointegrative properties, measured by μ CT, in the setting of infection were greatest in TPS implants; however histologic analysis showed greatest BIC% in TiNT+Ag implants as well as greater cortical connectivity (contiguous bone between bone-implant interface and cortical shell) in the nanotube cohorts. Ti showed the lowest GP% in both the non-TC and TC cohorts, followed by TiNT+Ag in the non-TC cohort and TiNT in the TC cohort.

REFERENCES

- Shokuhfar T, Hamlekhan A, Chang J-Y, et al. "Biophysical Evaluation of Cells on Nanotubular Surfaces: The Effects of Atomic Ordering and Chemistry," International Journal of Nanomedicine, Online Aug 2014, Vol. 9, No. 1, pp. 3737-3748.

Work funded through the University of Michigan MTRAC for Life Sciences Innovation Hub (Subcontract #3004361821).